Future Technology
Open Access Journal
ISSN 2832-0379

February 2024| Volume 03 | Issue 01 | Pages 01-12

Journal homepage: https://fupubco.com/futech

https://doi.org/10.55670/fpll.futech.3.1.1

Future Publishing LLC

Article

Environmental assessment and CO_2 emissions of Brayton cycle configurations based on exergo-sustainability, economic and ecological efficiency using multi-criteria optimization technique

Fidelis I. Abam[1]*, Bassey B. Okon[2], Isuamfon. F. Edem[2], Macmanus C. Ndukwu[3], Ene. B. Ekpo[4], Ogheneruona E. Diemuodeke[5]

[1]Energy, Exergy and Environment Research Group (EEERG) Department of Mechanical Engineering, University of Calabar, Calabar Nigeria
[2]Department of Mechanical Engineering, Akwa Ibom State University, Ikot-Akpaden, Nigeria
[3]Department of Agricultural and Bioresources Engineering, Michael Okpara University of Agriculture Umudike, P.M.B.,7267, Umuahia, Nigeria
[4]Department of Mechanical Engineering, Cross River University of Technology, Calabar, Nigeria
[5]Energy and Thermofluid Research Group, Department of Mechanical Engineering, Faculty of Engineering, University of Port Harcourt, PMB 5323, Choba, Port Harcourt, Rivers State, Nigeria

ARTICLE INFO

Article history:
Received 19 March 2023
Received in revised form
18 April 2023
Accepted 22 April 2023

Keywords:
Gas turbine, Sustainability, Energy efficiency, CO_2 emissions, Exergoenvironmental

*Corresponding author
Email address:
fidelisabam@unical.edu.ng

DOI: 10.55670/fpll.futech.3.1.1

ABSTRACT

The performance indicators of Brayton cycle configurations (BCY) for the topping cycle application are presented. The indicators include exergy efficiency, ecological efficiency, sustainability index, environmental impact, and economic parameters. The study's objective is to access the key indicators of sustainability and investment cost to provide valid information for the choice of GT configuration as topping cycles. Five BCY configurations (Model 1 to Model 5) were studied. The maximum exergy efficiency of 28 % was obtained across the studied models. In addition, the waste exergy ratios, environmental effect factors, and CO_2 emissions were determined for each model. The CO_2 emissions were found to vary from 102.8 to 168 kg/MWh. Model 1 and Model 5 had the highest payback periods of 2.3 and 3.6 years, respectively, with the least unit cost of energy. Similarly, the highest cost of investment was obtained with Model 5. Results from the TOPPIS analysis show that the closeness to the final positive ideal solution varied from 0.218 to 0. 56 across the BCYs. The best model close to ideality was model 5 and thus ranked first and based principally on economic, technical, and environmental sustainability. Furthermore, the optimization results show that there are prospects for system retrofitting.

1. Introduction

Renewable Climate change and conventional energy resource depletion have increased the need for integrating different energy production entities to achieve a common prime energy input. In power-generating plants such as gas turbine (GT) plants. Fossil-based fuels are the prime energy input for electricity production. In contrast, the waste exhaust heat from the flue gasses can be employed to power bottoming cycles, including organic Rankine cycles (ORC), absorption refrigeration systems, heating units, and desalination cycles. Additionally, in recent times, integrated multi or poly-energy generation with a gas turbine (Brayton cycle) as the topping cycle has gained a wider interest in the energy generation industries. Many scholars have presented studies on simple and complex thermal plants. Some Brayton cycle configurations are employed as topping cycles to power bottoming subsystems. For example, Mohan et al. [1] developed and examined a combined energy-generating system that utilizes the waste exhaust heat from a Brayton cycle (BCY) to produce electric energy from an ORC

Nomenclature:

c	specific cost
$\dot{E}x$	rate of exergy transfer, (kW)
$\dot{E}x_D$	rate of exergy transfer, (kW)
i	interest rate, (%)
$\dot{m}$	rate of mass transfer, (kg/s)
$\dot{Q}$	rate of heat transfer, (kW)
T	temperature, (K)
w	parameter weighting, (-)
$\dot{W}$	rate of work transfer, (kW)
Z	equipment cost, ($)

Greek symbols:

ψ	exergy efficiency
λ	mean of priority vector
Ø	fuel calorific value

Abbreviations

BCY	Brayton cycle
CC	combustion chamber
ECF	ecological efficiency
EEF	environmental effect factor
ESI	exergetic sustainability index
GT	gas turbine
HPC	high power compressor
HPT	high power turbine
LPC	low power compressor
LPT	low power turbine
ORC	organic Rankine cycle
PBP	payback period
TOPSIS	Technique for Order of Preference by Similarity to the Ideal Solution
UCOE	unit cost of energy
WER	waste exergy ratio

concurrently; water from a desalination plant and cooling from a vapor absorption refrigeration system. The BCY contains a high-power turbine and a reheat system that drives a free turbine. The analysis was based on technical and economic assessments. The obtained results indicate that the integrated system recorded efficiency of approximately 85 %, CO_2 emission reduction per MWh of about 51.5%, life cycle cost of $66 million, and a break-even period of 1.38 years. Njoku et al. [2] presented an integrated system that comprises an ORC, an absorption refrigeration cycle, and a BCY. The study utilizes waste exhaust heat from three parallel toppings BCYs to drive the subsystems. The results show that the overall power output from the integrated plant increased by about 9.1 %, with about a 13.3 % maximum reduction in fuel consumption and, most importantly, an increase in the sustainability index of nearly 8.4 %. A similar study was presented by Oko and Njoku [3], where waste exhaust heat from parallel topping BCYs was used to drive two subsystems, a Rankine cycle with an organic Rankine cycle. Different working fluids for the ORC were examined. The results indicated a 12.4 MW increase in the power output by reducing the flue gas temperature from 126 to 100^{0}C. Further studies by Moharamian et al. [4] proposed an integrated system with hydrogen addition in the combustion chamber of an externally fired biomass single shaft topping BCY. The integrated system was designed for heat, electricity, and hydrogen production. The study inferred that the hydrogen addition to the combustion chamber reduced the fuel consumption rate by 27%. The exergy destruction cost rate and the exergy loss were reduced by 78 % and 10%, respectively. A similar study was performed by Khalid et al. [5] for biomass-fired single shaft topping BCY integrated with a solar system for multi-energy production. The results show that the proposed system recorded an overall energy efficiency of 66.5%, with 39.7 % for exergy efficiency. Also, the energy and exergy efficiencies stood at 64.5 and 37.6%, respectively, when the biomass-fired BCY operated alone. At the same time, 27.3% energy efficiency and 44.3 % exergy efficiency were calculated when the solar system operated alone. Furthermore, Maheshwaria and Singhb [6] presented eight different intercooler gas turbine-based combined cycle configurations. The configurations of the combined plant vary based on the cooling medium. The mediums used for intercooling are either ammonia-water or steam, intercooling, single/dual/triple pressure heat recovery steam generator, steam turbine, reheating, or ammonia water turbine. The results confirm that maximum work of 1142 kJ/kg can be achieved for about 0.6 ammonia concentration. In contrast, for the concentration of 0.7, about 53.87% and 58.46 are achieved for energy and exergy efficiencies. Other studies by Abam et al. [7] developed an integrated multigeneration comprising a Brayton cycle, a Rankine cycle, ORC for power and cooling production, a Kalina cycle for power generation and cooling, and a lithium-bromide vapor absorption cycle for cooling. The topping cycle is an intercooled BCY with supplemental firing. The study obtained a total power output of 183 MW. Also, maximum exergy efficiency and specific CO_2 emission of 61.50 % and 3.0×10^{-7} kg/MWh were achieved with a unit cost of energy estimated at 0.0166 $/kWh. Additionally, sustainability refers to the capacity to supply energy resources in a sustainable and available manner at an equitable cost, resulting in no or negligible negative impact. Exergy assessment is a prolific tool that can be applied to measure the degree of sustainability of an energy system. In recent times, exergetic sustainability, an extended form of exergy analysis, has been applied to studying different thermal systems. For example, Aydin [8] studied the exergetic sustainability indicators (ESI) of two configurations of an LM6000 gas turbine engine. The following ESIs were considered exergy efficiency, exergy recovery ratio, exergy destruction factor, environmental effect value or factor, waste exergy ratio, and sustainability index. The study established the degree of sustainability for the two considered cases of LM6000 GT systems. The study of Balli and Hepbasli [9] presented the economic, sustainability, and environmental cost damage of a T56 turboprop GT engine. The exergetic sustainability limit of the T56 turboprop system was determined, followed by the environmental damaged cost, which stood at 423.94 $/h and 576.97 $/h for 75 and 100% mode of operations, respectively. Further analysis obtained about 634.93 $/h and 665.85 $/h at military and Take-off modes. The study's novelty was that environmental cost damage and sustainability levels were established for different operational modes. The latter gave

design engineers and power plant operators a clear insight into the good design and operational parameters for environmental sustainability. The sustainability of turboprop engines for different flight phases has been presented [10]. In this study, two phases taxing and landing, were considered. The phases of landing and taxing had minimum exergy efficiency and exergetic sustainability not greater than 20.6 % and 0.26, respectively. The study inferred that the exergy waste ratio and the sustainability values of the system were substantial at the climb, maximum, normal/maximum, cruise/continuous take-off, and automatic power reverse stages. The concept of exergetic sustainability has been applied equally to different energy systems (renewable) and systems where BCY is not the topping cycle. These included the studies of Haroon et al. [11], which presented an exergetic sustainability, exergo-environmental, and economic of a GT bottoming power plant operating with a CO_2-based dual mixture. The environmental impact and improvement indicators and exergy-based stability factors were considered. The maximum exergo environmental impact factor of 0.667 and 0.2 sustainability index were obtained. The extended application for renewable systems includes Midilli and Dincer [12], who estimated a fuel cell's environmental impact and sustainability. The study obtained a maximum environmental destruction factor or the coefficient of 3.42 and an exergy-based stability factor of 0.728. The work of Jankowski and Borsukiewicz [13] considered the exergy-based sustainability indicators for an ORC. All minimum values of the waste exergy ratio and environmental effect factor are obtained at an evaporation temperature of 75^{0}C. Similarly, Abam et al. [14] presented thermo-sustainability indicators for different ORC configurations operated with different working fluids. The study observed that the differences in the thermodynamic inputs parameters affect, to a large extent, the thermo-sustainability indicators. The environmental effect factor for the configurations was between 1.05 and 1.16, with minimum values obtained using R245fa refrigerant.

2. Study objective and contribution

Understanding thermal system operation will help administrators make energy policies on appropriately harnessing resources for sustainability and a low-carbon future. From the reviewed studies, no data could form a basis for selecting BCY topping configuration for bottoming operations, which describes exergetic sustainability, environmental sustainability, economic cost, and ecological parameters under some operating conditions. Again, only technical and socio-economics factors may not offer a comprehensive guide to the future energy transition. For these reasons, thermal systems operating in some closed environmental conditions with different considerations can be ranked through a multi-criterion technique to ascertain the most sustainable system. However, in this study, the thermo-sustainability indicators for different configurations of Brayton topping cycles for bottoming applications are described and ranked based on a multi-criteria decision analysis. The specifics of the study include the determination of the waste exergy ratios, environmental effect factors, life cycle cost, payback period, and ecological efficiency. The study, in this case, is considered noteworthy as generated data may form a basis for more complex system analysis and optimization.

3. Methodology and model formulation

3.1 System configuration

Five different Brayton cycles for topping cycle application as shown in Figure 1 (a-e). The GTs cycle configuration has different combinations of components: an air compressor (AC), combustion chamber (CC), gas turbine unit (GTU), heat exchanger (HEX), and an intercooler. Model 1 (Figure 1a) shows a simple gas turbine plant with an air compressor, combustor, and turbine unit. Model 2 (Figure 1b) has a high-pressure turbine (HPT) which drives the air compressor, and a free power turbine (FPT) for power generation. Model 3 (Figure 1c) is incorporated with an intercooler for reducing the mechanical work requirement of the air compressor and a heat exchanger for regeneration for increasing the enthalpy of the compressed air before combustion. Model 4 (Figure 1d) is integrated with a heat exchanger to increase the enthalpy of the compressed air. But the configuration is generic. Model 5 (Figure 1.e) is integrated with an additional combustor for reheating to effect intercooling and reheating simultaneously.

3.2 System description

In Figure 1a, atmospheric air enters state 1 and is compressed to state 2, where it enters the combustion chamber (CC), mixing with the fuel. The burnt gasses expand in the turbine at state 3, where expansion occurs in the turbine. In Figure 1b, the burnt gasses from the combustion chamber at state 3 expand first in a high-power turbine (HPT). The second expansion is completed in a low power turbine (LPT) at state 3. In Figure 1c, the compressed air is cooled in the intercooler at state 2 before recompression at state 3 in the high power compressor (HPC) at state 3. The compressed air from the HPC enters the CC for atomization and combustion. The burnt gasses expand, thus producing power. In Figure 1d, the compressed air passes through the heat exchanger before the combustion chamber and expansion in the turbine. In Figure 1e, part of the exhaust gas from the HPT is used to reheat the mixture in the reheater before expansion in the LPT.

3.3 Thermodynamic modelling

The first law of thermodynamics and the second law were applied to analyzing the cycles. Furthermore, to achieve the objectives of this study, the following assumptions were made: The system was evaluated under steady-state conditions. The properties of air were considered as possessing ideal gas characteristics. The system is assumed to have adiabatic boundaries such that the heat losses to the environment are negligible. The systems were assumed to operate without any pressure drops. The isentropic efficiencies of the turbines and compressors are constant during their life cycle. The temperature and pressure at the inlet to the system are taken at ambient conditions. For the systems having intercoolers, the intercooling is assumed to be perfect in between compressors. The effect of potential and kinetic energies are neglected in the system [15, 16]. The energy flow balance for the components can be written in terms of the steady-state stream equation for the $\mathbf{k^{th}}$ component [15] as:

$$\sum \dot{m}_i = \sum \dot{m}_0 \quad (1)$$

$$\sum \dot{Q}_k + \sum \dot{m}_i \left(h_1 + \frac{C_i^2}{2} + gz_1\right) = \sum \dot{m}_e \left(h_0 + \frac{C_0^2}{2} + gz_0\right) + \sum W \quad (2)$$

$$\dot{E}_{xd} = \sum_k \left(1 - \frac{T_0}{T_k}\right) \dot{Q}_k - \dot{W}_{cv} + \sum_i \left(n_i \dot{E}x_i\right) - \sum_e \left(n_e \dot{E}x_e\right) \quad (3)$$

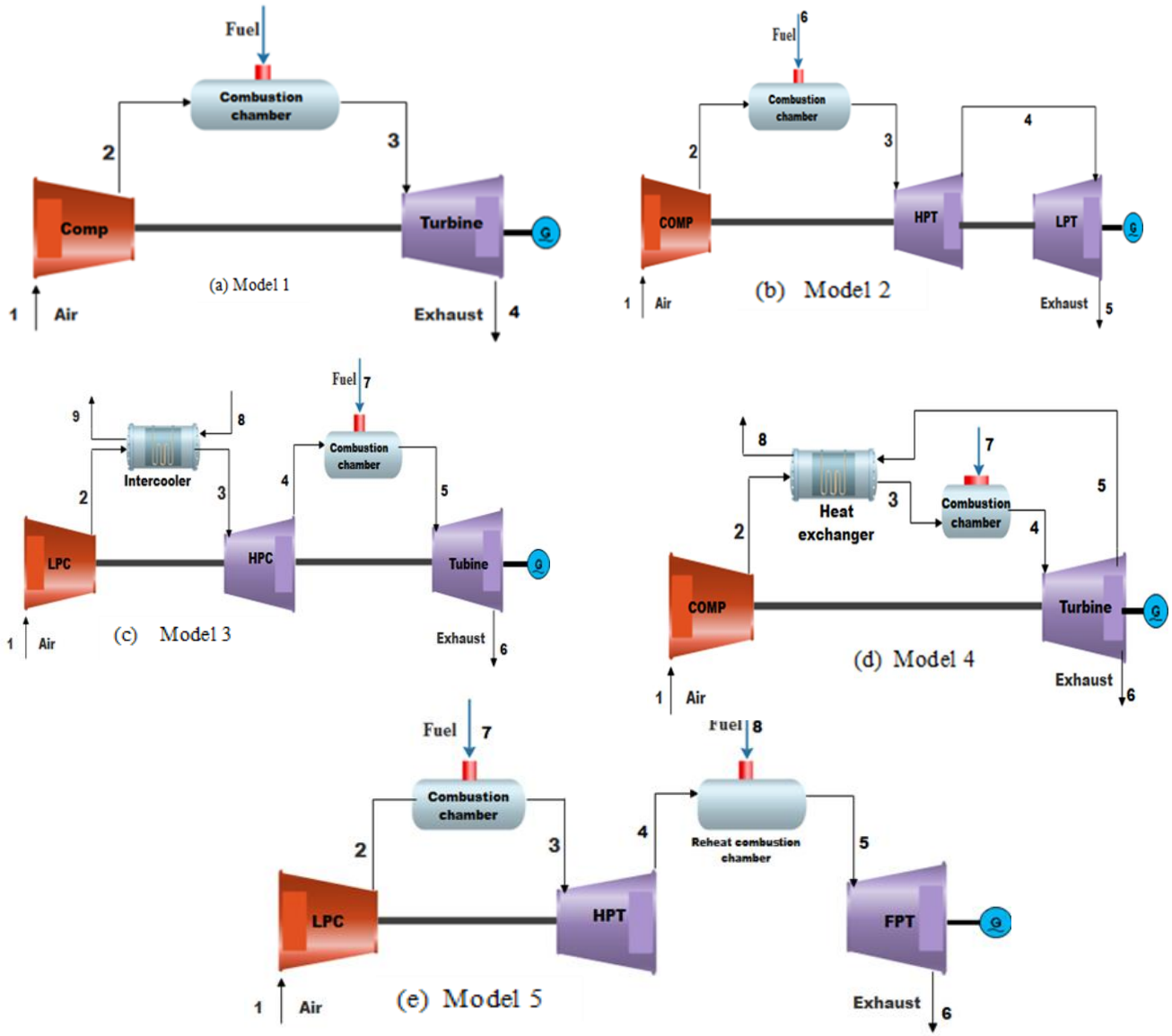

Figure 1. Different configurations of the Brayton cycle for bottoming cycle operations

Where the rate of heat input to the system and the mass influx are denoted as $\dot{Q}_k$ and$\dot{m}_i$, respectively. Further, the enthalpy, kinetic energy, and potential energy of the stream are denoted as h_1, $\frac{C_i^2}{2}$, and gz_1, Where $\dot{E}_{xd}$ is the exergy destruction rate, $\left(1-\frac{T_0}{T_k}\right)\dot{Q}_k$ is the exergy flow rate accompanied by heat transfer, $\dot{W}_{cv}$ is the rate of work done within the control volume, $n_i\dot{E}x_i$ and $n_e\dot{E}x_e$ is the exergy flow rate in and out of the control volume. Moreover, for a specific component, the exergy destruction can be expressed in terms of product and fuel as:

$$\dot{E}_{D,k} = \dot{E}_{F,k} - \dot{E}_{Pk-}\dot{E}_{L,k} \quad (4)$$

The exergy efficiency,ψ_k And the exergy destruction ratio is equally defined for the **kth** component as:

$$\psi_k = \frac{\dot{E}_{Pk}}{\dot{E}_{F,k}} \quad (5)$$

$$Y_{D,k} = \frac{\dot{E}_{D,k}}{\dot{E}_{F,total}} \quad (6)$$

3.4 Sustainability exergy efficiency and environmental indicators

The exergetic efficiency of the gas turbine plant is defined as the ratio of exergy of turbine work to fuel exergy expressed generally as in Eq. (7). Similarly, Eq. (7) is applied to develop the overall exergy efficiencies for the BCY models expressed in Eqs. (7)- (12)

$$\psi_{GT.plant} = \frac{E_{x,w}}{E_{xfuel}} = \frac{W_{GT}}{E_{x,fuel}} \quad (7)$$

$$\psi_{plant\ model\ 1} = \frac{W_T - W_C}{m_{fTOTAL}\sum x_k\bar{e}_k^{CH} + \bar{R}T_0\sum x_k \ln x_k} \quad (8)$$

$$\psi_{plant\ model\ 2} = \frac{W_{HPT} + W_{HPT} - W_C}{m_{fTOTAL}\sum x_k\bar{e}_k^{CH} + \bar{R}T_0\sum x_k \ln x_k} \quad (9)$$

$$\psi_{plant\ model\ 3} = \frac{W_T - W_{HPT} - W_{LPC}}{m_{fTOTAL}\sum x_k\bar{e}_k^{CH} + \bar{R}T_0\sum x_k \ln x_k} \quad (10)$$

$$\psi_{\text{plant model 4}} = \frac{W_T - W_C}{m_{fTOTAL} \sum x_k \bar{e}_k^{CH} + \bar{R}T_0 \sum x_k \ln x_k} \quad (11)$$

$$\psi_{\text{plant model 5}} = \frac{W_{HPT} + W_{LPT} - W_C}{m_{fTOTAL} \sum x_k \bar{e}_k^{CH} + \bar{R}T_0 \sum x_k \ln x_k} \quad (12)$$

3.5 Exergetic sustainability index

The exergetic sustainability index is the reciprocal of the environmental effect factor. The range of this index is between 0 and ∞ [16]. The exergetic sustainability index is a non-dimensional term that explains how an energy conversion system's total useful output exceeds the total internal thermodynamic irreversibilities. The index assesses the fraction of a system's useful work that overcomes the system's inherent net exergy destruction. Thus, a system with exergy output far larger than the total destruction rate will have 'sustainabilities' greater than unity, while systems with comparatively large destruction at par with the plant output are not sustainable. Appropriately, the reciprocal of the environmental effect factor is termed the exergetic sustainability index and provides a platform for comparison between the environmental degradation due to exergetic output from each system [16].

$$ESI = {}^{1}/_{\Gamma_{eef}} \quad (13)$$

3.6 Waste exergy ratio

The waste exergy ratio quantifies the degree of cumulative thermodynamic irreversibilities in a plant with respect to the available external exergy input to the system. The waste exergy ratio is obtained mathematically as the overall exergy waste (or destruction) for the system on the total exergy input [17].

$$\Gamma_w = \frac{\sum \dot{E}_{waste}}{\dot{E}_{fuel}} \quad (14)$$

3.7 Environmental effect factor

The environmental effect factor, Γ_{eef} quantifies the degree of cumulative thermodynamic irreversibilities in a plant with respect to the plant's net exergy efficiency. It also relates to how a useful plant output is severely affected due to irreversibilities resulting in environmental concerns. The Γ_{eef} is obtained as the waste exergy ratio upon the exergy efficiency expressed in [17].

$$\Gamma_{eef} = \frac{\Gamma_{w,e}}{\psi_{GT}} = \frac{E_{waste}}{W_{GT}} \quad (15)$$

3.8 Ecological efficiency

The ecologic efficiency is an indicator that allows assessing the thermoelectric power plant gaseous emission environment impact by comparing the hypothetically integrated pollutant emissions to the existing air quality patterns. It helps assess the pollution rate in a plant, considering the combustion of one kg of fuel. The volume of gases exited per unit of energy produced is presented with the expression [18].

$$\varepsilon = \sqrt{\left[\frac{0.204\eta}{\eta + \Pi_g} \ln\left(135 - \Pi_g\right)\right]} \quad (16)$$

Where Π_g is the pollutant indicator value and alternates between 0 and 1, while η is the efficiency of the power plant. The pollutant indicator, Π_g is defined in reference [18].

$$\Pi_g = \frac{(CO_2)_e}{\emptyset_i} \quad (17)$$

Where $(CO_2)_e$ in kg/kg (kg per kg of fuel) is the equivalent carbon dioxide obtained from the burning fuel, $\emptyset_i$ (MJ/kg), is the fuel lower calorific power and Π_g (kg/MJ), is the pollution indicator. For calculation of the equivalent carbon dioxide coefficient, the CO_2 the maximum concentration value allowed is divided by the corresponding air quality patterns for NO_X, SO_2 and PM. Thus, the expression for the equivalent CO_2 emissions is as follows:

$$(CO_2)_e = (CO_2) + 80(SO_2) + 50(NO_X) + 67(PM) \quad (18)$$

Details for determining carbon dioxide emissions, sulfur, nitrogen, and particulate matter [19]. Additionally, using Eqs. (17) and (18), the mass, energy, and exergy balances are established for the components and exergy efficiency.

3.9 Economic evaluation

The typical exergoeconomic equation for a thermal energy conversion plant is expressed as:

$$c_{q,k}\dot{E}_{q,k} + \sum_i \left(c_i \dot{E}_i\right)_k + \dot{Z}_k = \sum_e \left(c_e \dot{E}_e\right)_k + c_{w,k}\dot{W}_k \quad (19)$$

Where $\sum_e \left(c_e \dot{E}_e\right)_k$ represents cost rates related to the exit streams of the k^{th} element; $c_{w,k}\dot{W}_k$ is the power generation cost rates of the k^{th} element; $c_{q,k}\dot{E}_{q,k}$ is the heat transfer cost rates of k^{th} component; $\sum_i \left(c_i \dot{E}_i\right)_k$ represents cost rates related to the entering streams of k^{th} component; $\dot{Z}_k$ is the cost rate of the capital investment of the k^{th} component, and c denote the specific cost. Similarly, the total cost rate for the k^{th} component ($\dot{z}_k$), is the summation of the entire capital investment and the operation and maintenance of the system k^{th} component, as presented in reference [20].

$$\dot{Z}_k = \dot{Z}_k^{CI} + \dot{Z}_k^{OM} \quad (20)$$

The yearly levelised capital investment for the component is estimated as in reference [20].

$$\dot{Z}_k = CRF \times \frac{\emptyset_k}{N \times 3600} \times Z_k \quad (21)$$

Where Z_k signifies the purchased cost of the equipment k, *N* is the operating hours of the component functions, ϕ_k, represents the maintenance factor, and CRF represents the capital recovery factor, as shown in Eq. (22).

$$CRF = \frac{i(1+i)^n}{(1+i)^n - 1} \quad (22)$$

The economic merit and other economic indicators are calculated from [20]. Consequently, the unit of electricity cost, UCOE ($/kWh), is estimated from Eq. (23).

$$UCOE = \frac{Z_{ALCC}}{365 \times E_{DP}} \quad (23)$$

Where E_{DP} the energy produced per day $\left(24 \times \dot{W}_{net}\right)$ and the Z_{ALCC} is presented as:

$$Z_{ALCC} = CRF \times Z_{LCC} \quad (24)$$

The payback period (PBP) is calculated from Eq. (25)

$$BEP = \frac{LCC}{C_{Tarrif} \times A_{EP}} \quad (25)$$

Where Z_{LCC}, Z_{ALCC}(\$), Z_i (\$), C_{Tarrif} (\$/kWh), A_{EP} (kWh/y) defines the life cycle cost, the selling price per unit of electricity, and the annual energy generated, respectively.

4. The multi-criteria optimization technique: the TOPSIS

The TOPSIS method was applied to select the optimal BCY technology from other alternatives from different operating parameters. The various configurations or alternatives comprise Model 1 to Model 5 specifications as defined earlier for this study. In contrast, the parameters include net power (MW), life cycle cost (LCC), the unit cost of energy (UCOE), payback period (PBP), Specific CO_2 emissions, exergy destruction, and environmental effect factor. The TOPSIS technique follows 6 steps and considers the relative distances of the positive and negative ideal solutions from the ideal solution [21]. The steps include:

Step 1: building a normalized decision matrix

The different system attributes are transformed into dimensionless attributes to allow for the comparison of the different attributes. Finally, the value of every criterion is divided by the considered norm of that criterion Eq. (26).

$$r_{ij} = \frac{x_{ij}}{\sqrt{x_{ij}^2}} \quad (26)$$

Step 2: building the weighted normalized decision matrix

Eq. (27) presents a weighted normalized matrix.

$$v_{ij} = w_i \times r_{ij}, i = 1,2,\dots,m;\ j = 1,2,\dots,n \quad (27)$$

Where, w_i is the weight vector obtained using the Analytical Hierarchy Program (AHP)?

Step 3: The determination of the ideal solutions (Both positive and negative solutions)

The positive ideal solution is presented in Eqs. (28) and (29)

$$A^+ = \{\max(v_{ij}) \,|i \in I, \min(v_{ij}) \,|i \in I'\} \quad (28)$$

$$A^+ = \{v_1^+, v_2^+, \dots, v_n^+\} \quad (29)$$

Where,

$I = \{i = 1,2,\dots,m | i \text{ is associated with benefit criteria}\}$

$I' = \{i = 1,2,\dots,m | i \text{ is associated with cost criteria}\}$

Likewise, the negative solution is presented in Eqs. (30) and (31).

$$A^- = \{\max(v_{ij}) \,|i \in I', \min(v_{ij}) \,|i \in I\} \quad (30)$$

$$A^- = \{v_1^-, v_2^-, \dots, v_n^-\} \quad (31)$$

Step 4: The determination of Euclidean distance

The separation between each alternative is got by the n-dimensional Euclidean distance as:

$$s_i^{\pm} = \sqrt{\sum_{j=1}^{n} \left(v_{ij} - v_i^{\pm}\right)^2} \quad (32)$$

where $i = 1, 2, 3, \dots, m$, represent the ith alternative.

Step 5: relative closeness to the ideal solution

The relative closeness existing between each of the alternatives to the ideal solution is estimated using Eq. (33).

$$c_i^+ = \frac{s_i^-}{s_i^+ + s_i^-} \quad (33)$$

Step 6: ranking of the alternatives

In ranking the alternatives, it is done in descending order of $c_i^+$with the highest c_i^+ .The value is given the order 1, the next 2, in that other. Similarly, the procedure in reference [22] was used to determine the weights applied in the TOPSIS.

5. Results and discussion

5.1 Thermodynamic parameters

The properties of the system have been modelled to facilitate computation of the performance index of the different GT configurations already shown in Figure 1. The input parameters used for the simulation include the compressor inlet temperature (298K), compressor inlet pressure (1.013 bar), the mass flow rate of air (427kg/s), and the mass flow rate of fuel (7.35kg/s) and turbine and compressor isentropic efficiencies (0.89). These input parameters were used to obtain the thermodynamic state points in Table 1. In addition, other sustainability and environmental indicators were calculated from these input parameters and the data in Table 1.

5.2 Thermodynamic performance of the overall plant

The overall performance of the plant models is depicted in Figure 2, which includes exergy destruction, improvement potential, and the exergy of product and fuel. The study shows that the models' exergy destruction (ED) ranged between $0.19 \leq ED \leq 0.279$ MW. Model 3 had the highest overall ED, followed by models 4 and 5. Similarly, exergy losses (EL) ranged between $0.45 \leq EL \leq 0.78$ MW. The largest EL were observed with model 5 and model 3, with values estimated at 0.78 and 0.66 MW, respectively. The significant exergy losses in model 5 are attributed to the large losses in the combustion and the reheat units. Studies have shown that exergy losses are dominant in the combustion chamber due to the large temperature variance between the flame and the combustion mixture [23]. However, model 5 shows the highest potential for improvement with a value of 0.45 MW. The exergy of the product and exergy of fuel are equally depicted in Figure 2, which is dominated by model 5.

5.3 Power output, specific CO_2 emissions, and environmental analysis

The models' power output and specific CO_2 emissions are presented in Figure 3 and Figure 4, respectively. The maximum output power of 118.89 MW is generated by model 5 with a corresponding specific CO_2 emission of 102.3 kg/MWh. The power output varies from 66.08 to 85.56 MW for the remaining models 1-4. Model 4, which generates a net power of 66.08 MW, produces 168 kg/MWh of CO_2 emissions, followed by Model 1 with specific CO_2 of 166.7 kg/MWh. Model1 and Model 4 are almost similar in configuration. The only variance is that Model 4 is integrated with a heat exchanger for regeneration. The results show that the integration of the regeneration system resulted in a 1.2 % increase in power and a 0.77 % decrease in specific CO_2 emissions.

Table 1. These input parameters used to obtain the thermodynamic state points

State point	m [kg/s]	h [kJ/kg]	s [kJ/kg.K]	T [K]	P [bar]	E [kW]
Model 1						
1	427.0	298.4	5.695	298.0	1.013	0
2	427.0	631.9	5.818	623.4	9.117	126754
3	434.3	1337.0	6.595	1250	9.117	334499
4	434.3	855.0	6.758	829.7	1.013	104221
5	7.348	42300	-	298.0	9.117	362541
Model 2						
1	427.0	298.4	5.695	298.0	1.013	0.0000
2	427.0	631.9	5.818	623.4	9.117	126754
3	434.3	1337.0	6.595	1250	9.117	334499
4	434.3	1009.0	6.683	967.2	2.388	180756
5	434.3	843.0	6.743	818.9	1.013	100902
6	7.348	42300	-	298.0	9.117	362541
Model 3						
1	427.0	298.4	5.695	298.0	1.013	0.0000
2	427.0	437.2	5.762	435.4	3.039	50687
3	427.0	313.5	5.429	313.0	3.039	40273
4	427.0	459.5	5.497	457.3	9.117	93993
5	436.1	1337.0	6.595	1250.0	9.117	335883
6	436.1	855.0	6.758	829.7	1.013	104652
7	9.145	42300	-	298.0	9.117	451201
8	20.3	104.2	5.695	298.0	1.013	0.0000
9	20.3	2706.0	7.434	388.0	1.013	42292
Model 4						
1	427.0	298.4	5.695	298.0	1.013	0.000
2	427.0	631.9	5.818	623.4	9.117	126754
3	427.0	793.1	6.05	773.4	9.117	166095
4	432.7	1337.0	6.595	1250	9.117	333206
5	432.7	855.0	6.758	829.7	1.013	103818
6	432.7	686.7	6.533	675.0	1.013	59944
7	5.669	42300.0	-	298.0	9.117	279670
Model 5						
1	427.00	298.4	5.695	298.0	1.013	0.000
2	427.00	631.9	5.818	623.4	9.117	126754
3	434.30	1337.0	6.595	1250.0	9.117	334499
4	434.30	1030.0	6.638	986.0	3.016	195875
5	437.60	1337.0	6.913	1250.0	3.016	295602
6	437.60	1044.0	6.965	998.0	1.013	160682
7	7.35	42300.0	-	298.0	9.117	362541
8	3.25	42300.0	-	298.0	3.016	159827

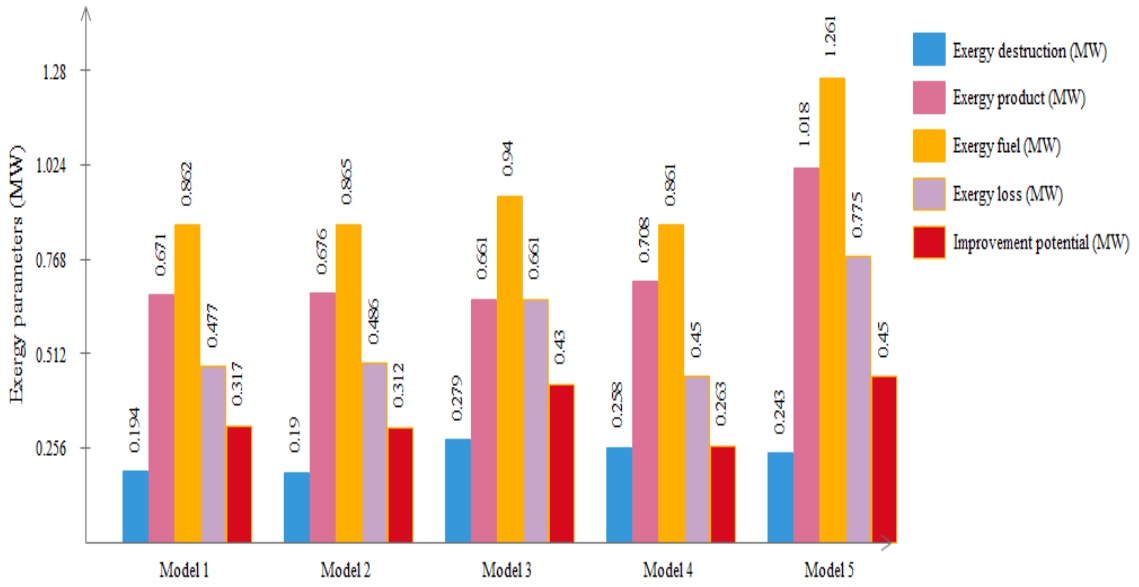

Figure 2. Overall exergy performance parameters for the BCY models

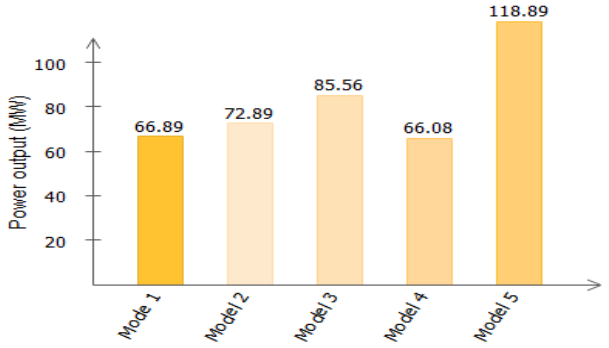

Figure 3. Net power output for the BCY models

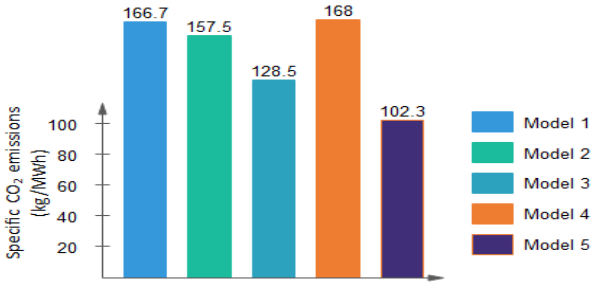

Figure 4. Specific CO_2 emissions for the different BCY models

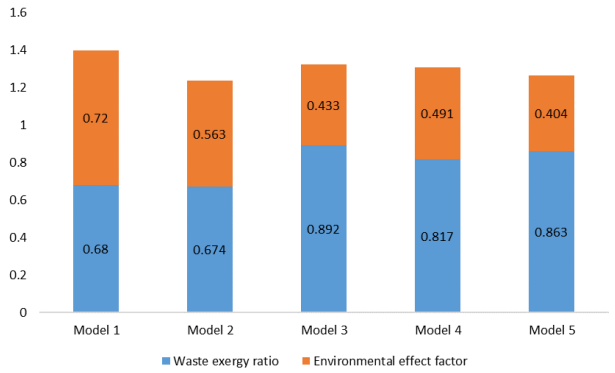

Figure 5. Exergeoenviromental parameters for the different BCY models

The exergeoenviromental parameters, waste exergy ratio, and environmental effect factor are presented in Figure 5. The waste exergy ratio (WER) and the environmental effect factor (EEF) ranged between $0.404 \leq WER \leq 0.72$ and $0.68 \leq EEF \leq 0.89$, respectively. The WER is maximum with Model 3 and Model 5 calculated at 0.82 and 0.89, respectively. The WER depends on the rate of exergy destruction, the exergy of fuel, and possibly the number of components. This is responsible for the high WER values observed in Models 3, 4 and 5. However, the payoff is in large work output (W_{GT}). Therefore, the EEF values depend mainly on W_{GT}. The EEF values for Model 3 and 5 are 0.491 and 0.404 with W_{GT} of 210.2 MW and 118.9 MW, respectively. Though the EEF is high for Model 3, this is a tradeoff with W_{GT}. The intercooler and the addition of HPC were responsible for the augmentation of the net power output. Similarly, the regeneration system in Model 5 was responsible for the decrease in EEF.

5.4 Comparison of ecological efficiency and performance indicators

The models' ecological efficiency (ECF), exergetic sustainability index (ESI), exergy efficiency, and energy efficiency are presented in Figure 6.

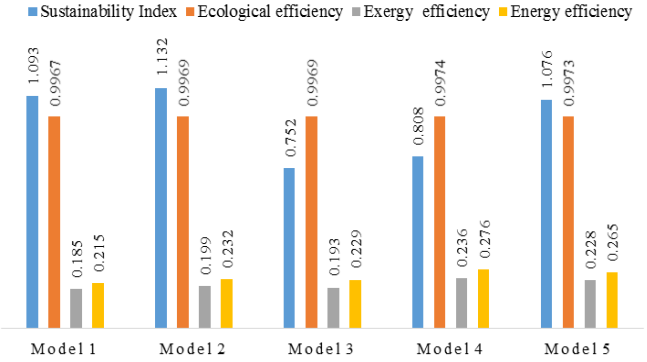

Figure 6. Comparison of ecological efficiency and performance indicators

The ECF ranged between $0.9967 \leq ECF \leq 0.9973$, while the ESI, exergy and energy efficiencies varied from 0.752 to 1.132, 18.50 to 23.60 % and 21.50 to 27. 60 %, respectively across the BCY models. The difference in ECF between models is about 0.02 % 0.05 %, and 0.06 % for Models1, 2 and 5 respectively. However, the difference between Models in terms of ECF is quite small. The ECF depends on the CO_2 emission rate and thermal discharge index [23]. Similarly, the exergy and energy efficiencies are highest in Models 4 and 5. The cause is ascribed to the rise in the inlet air temperature to the combustion chamber. The latter enhances combustion, thus producing high combustion exit temperature. From Carnot efficiency$\left(1-\frac{T_L}{T_H}\right)$, the ratio $\frac{T_L}{T_H}$ becomes small for high T_H. Thus, resulting in high Carnot efficiency.

5.5 Sensitivity and exergoeconomic analysis

5.5.1 Effect of dead state temperature on sustainability indicators

The effect of dead state temperature on exergy efficiency, ECF, and ESI are presented in Figure 7. The results indicate that the ECF decreases slightly with increased dead state temperature. For every one-degree rise in temperature, the ECF reduces by approximately 0.2 %, which implies that the environment is negatively affected by this amount. Similarly, the ESI decreases from 1.09 to 0.8397 for a degree rise in dead state temperature (DST) from 298 to 304 K. Also, the ESI decreases by 0.30 % for the one-degree increase in DST, while ESI reduces by 0.34 %. The DAT has a high effect on sustainability indicators for all the BCY models.

5.5.2 Effect of compressor and turbine isentropic efficiencies on ECF

Isentropic efficiencies of the compressor and turbine were investigated on the plant's ecological efficiency, with the results shown in Figure 8. Between turbine isentropic efficiencies of 0.72 and 0.88, the ecological efficiencies increased from 0.92 to 0.96. This corresponding increase results from higher isentropic efficiencies of the compressor and turbine. The latter results in low compressor work

requirements and improved turbine output. The cumulative effect results in highly increased turbine energy efficiency and ecological efficiency.

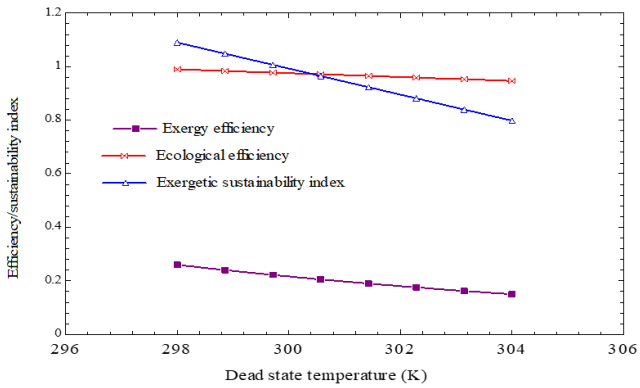

Figure 7. Effect of dead state temperature on sustainability indicators

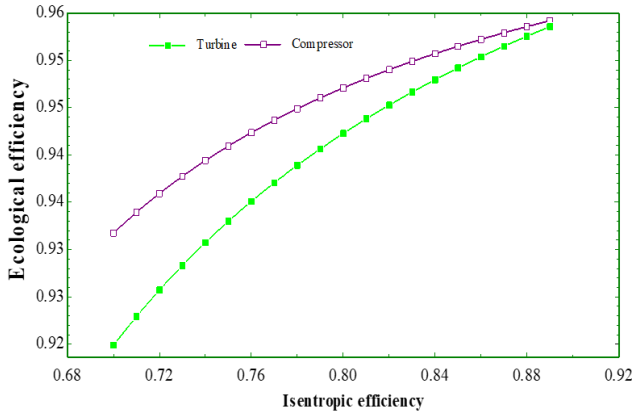

Figure 8. Effect of turbine and compressor isentropic efficiencies on ecological efficiency

5.5.3 Effect of compressor and turbine pressure ratios on ECF

Figure 9 shows the effect of compressor and turbine pressure ratios on ecological efficiencies. The results show that a higher compressor pressure ratio results in a decrease in ECF. This can be attributed to higher compressor work requirements at high-pressure ratios. Furthermore, high compressor pressure ratios limit the net turbine output, reducing the net energy efficiency at constant heat input. In contrast, high ecological efficiency values were recorded as turbine pressure ratios increased. This is because the gross work output of the turbine can be significantly enhanced when the pressure at the inlet to the turbine is raised at a constant temperature. Also, a large pressure gradient increases energy efficiency and results in high ecological efficiency.

5.5.4 Results of the economic analysis

The results of the economic analysis are presented in Table 2 for all the BCY models. The highest investment cost was obtained with Model 5. The total life cycle investment cost for model 5 was estimated at 2.91×10^5\$ with UCOE of 0.285 \$/kW and PBP of 3.6 years. Model 3 has a total investment cost 2.79×10^5\$, UCOE 0.0356 \$/kW with PBP of 3.5 years. Based on the investment cost and PBP, ordinarily, an investor will prefer Model 1, having a short investment period and quick recovery time. However, since the sustainability, economic, and other environmental considerations are involved in the choice, further analysis will be imperative to ascertain the best system close to the ideal solution. The succeeding results stipulate the outcome based on a multi-criteria approach for choosing the optimal model.

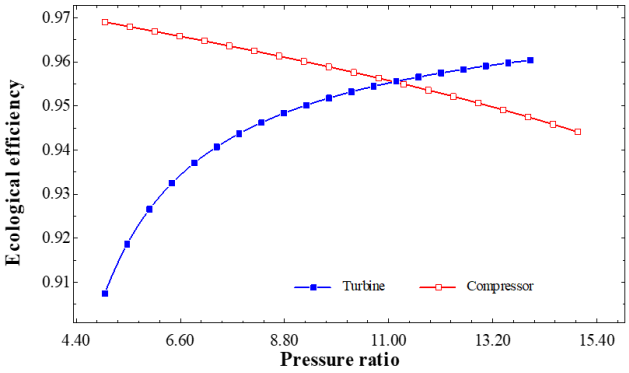

Figure 9. Effect of turbine and compressor pressure ratio on ecological efficiency

Table 2. Economic analysis of the GT models

S/N	LCC\$	UCOE (\$/kW)	PBP (Years)
Model 1	1.5×10^5	0.0294	2.3
Model 2	2.54×10^5	0.0401	3.45
Model 3	2.79×10^5	0.0356	3.5
Model 4	2.47×10^5	0.0426	3.4
Model 5	2.91×10^5	0.0285	3.6

5.5.5 Ranking based on multi-criteria decision optimization technique

The results obtained from the step-by-step procedure to obtain the exact closeness final positive ideal solution are presented in Figure 10 (a-f). Similarly, Figures (a-e) depict the procedural steps, while Figure 10f (step 6) is the final closeness results which will form the basis of choice for further analysis. The BCY configuration (Model1 to Model 5) Figure 10f is the last model ranking close to the ideal solution. From Figure 10f, the model ranking is based on environmental, economic and technical parameters. These parameters included the net power output, life cycle cost (LCC), the unit cost of energy (UCOE), specific CO_2 emissions, exergy destruction (ED) and environmental effect factor. The consideration for the ranking was based on the BCY model, which is comparatively flanking the ideal solution. Model 5 (Figure 10f) was close to the perfect solution in this study, consequently ranked as the first. This is followed by BCY Model 1, Model 3, Model 2 and Model 4. The parameters that make the best ranking of Model 5 include low specific CO_2 emission, high net power output and low environmental effect factor.

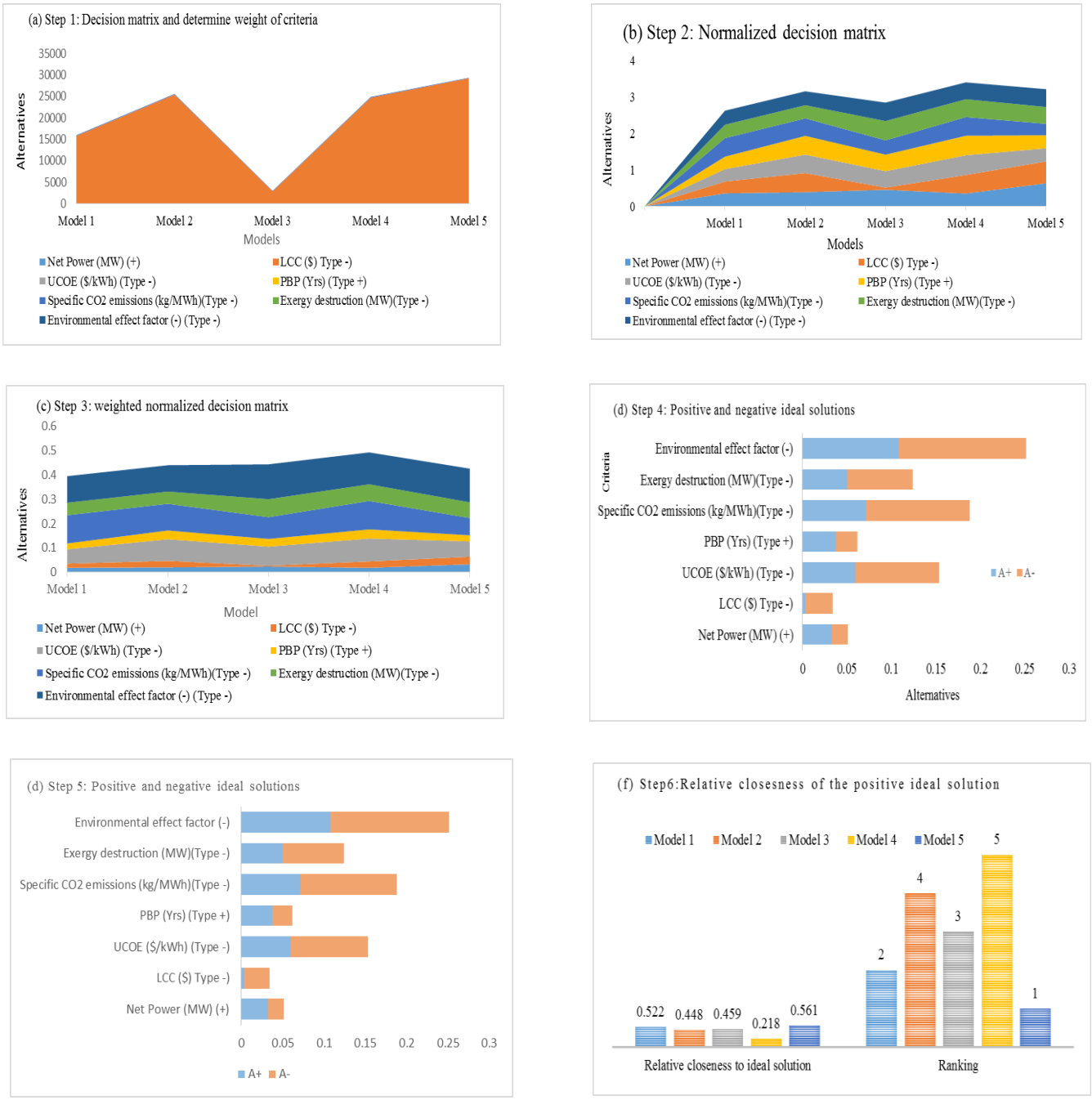

Figure 10. Procedure for determining the weights used in the TOPSIS analysis

The value for the relative closeness to ideality was highest for model 5, calculated at 0.561, followed by Model 1 with a value estimated at 0.52. Additionally, from Table 2, the LCC and PBP for Model 5 are the highest estimated at $2.91 \times 10^5$$ and 3.6 years, respectively, but the low specific CO_2 emissions, and environmental effect factor and UCOE can be a tradeoff. The results obtained can serve as a pointer for informed policy, proposing the necessity of other retrofitting technologies for the BCYs.

5.5.6 Parametric simulation of the optimum configuration (Model 5)

Figure 11 and Figure 12 present the optimum BCY configuration (Model 5).

In Figure 11, the combustion temperature effect on EEF and the specific CO_2 emission (SCM) is illustrated.The EEF and the specific CO_2 emission decreases with increasing combustion temperature by 13.9 % and 20.38 %, respectively. Similarly, Figure 12 depicts the effect of combustion temperature on the UCOE and net power output. The UCOE and the net power output decrease with increasing combustion temperature. The latter is possibly ascribed to the high power output resulting from the absence of the compressor work. On the other hand, high flue gases temperature does more valuable work in the turbine. Though a high-performance efficiency is required, operating the plant at a high temperature beyond the practical obtainable temperature limit results in high thermal implications.

Consequently, a tradeoff between environmental sustainability and economics is imperative.

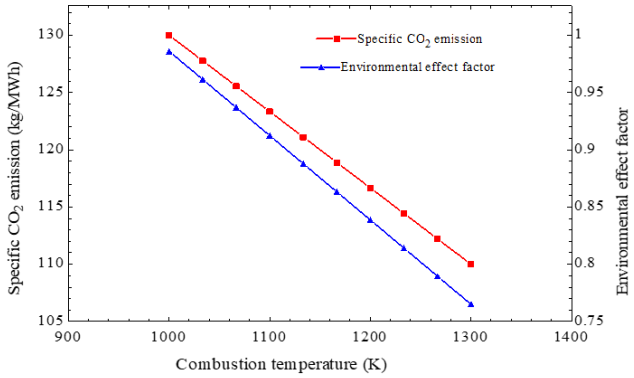

Figure 11. Effect of combustion temperature on EEF and specific CO_2 emissions

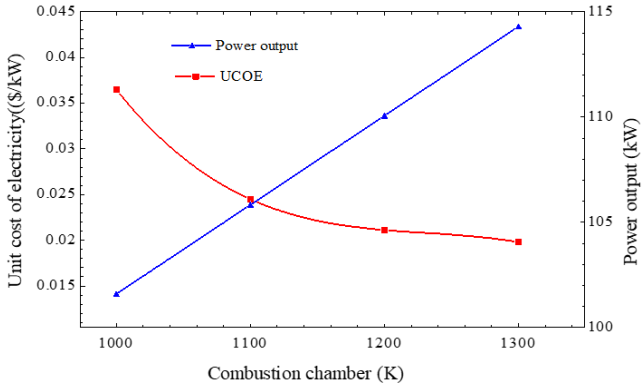

Figure 12. Effect of combustion temperature on power output and UCOE

6. Conclusion

The exergo-sustainability, economic and ecological efficiencies of gas turbine configurations for topping cycle applications were carried out in this study. The study presented different gas turbine models for possible topping cycles to run downstream or bottoming cycles. The technical reasoning is that data regarding sustainability, environmental impact, economic and carbon footprint should be paramount before considering topping cycles for bottoming operations. The study presented Five GT model configurations. The results show that Model 1, the generic cycle, had an improvement potential of 0.32 MW with ecological efficiency and sustainability index of 0.997 and 1.09, respectively. The waste exergy ratios and environmental effect factors across the models ranged between $0.404 \leq WER \leq 0.72$ and $0.68 \leq EEF \leq 0.89$ in that order. However, the exergeoenviromental parameters were less in Model 3 and Model 5, with overall exergy destruction of 279.50MW and 258.15MW, respectively. Similarly, the exergy of the product was highest in Model 5 and less in Model 1 and Model 3, calculated at 1.02 MW, 0.67MW, and 0.66 MW, respectively. The study inferred that understanding environmental parameters, economics, and sustainability are paramount for topping cycle choices to maintain economic and environmental sustainability. However, from the TOPSIS analysis, the models were ranked based on the following parameters: the net Power output, life cycle cost (LCC), the unit cost of energy (UCOE), specific CO_2 emissions, exergy destruction (ED), and environmental effect factor. The closeness to the final positive ideal solution for the models ranged between 0.218 and 0.561. Model 5 had the highest value and ranked first. The generated data can be used as a measure for feature system retrofitting.

Ethical issue

The authors are aware of and comply with best practices in publication ethics, specifically with regard to authorship (avoidance of guest authorship), dual submission, manipulation of figures, competing interests, and compliance with policies on research ethics. The authors adhere to publication requirements that the submitted work is original and has not been published elsewhere.

Data availability statement

Datasets analyzed during the current study are available and can be given following a reasonable request from the corresponding author.

Conflict of interest

The authors declare no potential conflict of interest.

References

[1] G. Mohan, S. Dahal, U. Kumar, A. Martin., H. Kayal. Development of natural gas fired combined cycle plant for tri-generation of power, cooling and clean water using waste heat recovery: Techno-economic analysis. Energies, 7(2014) 6358-6381.doi: 10.3390/en7106358.

[2] I.H. Njoku, C.O.C Oko, J.C. Ofodu. Performance evaluation of a combined cycle power plant integrated with organic Rankine cycle and absorption refrigeration system. Cogent Engineering 5(2018) 1451426. https://doi.org/10.1080/23311916.2018.1451426

[3] C. O. C Oko, I. H Njoku. Performance analysis of an integrated gas-, steam- and organic fluid-cycle thermal power plant. Energy 122(2017) 31-443.doi:10.1016/j. energy.2017.01.107.

[4] A. Moharamian, S. Soltani, M. A. Rosen, S. M Mahmoudi. (2017). Exergoeconomic and thermodynamic analyses of an externally fired combined cycle with hydrogen and injection to the combustion chamber. Inter J Hydrogen (2017)1-12.doi: https://doi.org/10.1016/j.ijhydene.2017.11.136

[5] F. Khalid, I. Dincer, M. Rosen. Energy and exergy analyses of a solar-biomass integrated cycle for multigeneration. Solar Energy 112(2015), 290-299.

[6] M. Maheshwaria, O. Singhb. Thermodynamic study of different configurations of gas- steam combined cycles employing intercooling and different means of cooling in topping cycle. Applied Therm Eng 169(2019) 114249.

[7] F. I Abam, E. D. Ogheneruona, E. B. Ekwe, A. Mohammed, D. S. Olusegun, A. K. Zafar., M. Imran, M. Farooq. Exergoeconomic and Environmental Modeling of Integrated Polygeneration Power Plant with Biomass-Based Syngas Supplemental Firing. Energies 13 (2020) 6018; doi: 10.3390/en13226018.

[8] H. Aydin. Exergetic sustainability analysis of LM6000 gas turbine power plant with steam cycle. Energy

57(2013)766-774.
http://dx.doi.org/10.1016/j.energy.2013.05.018.

[9] O. Balli, A. A. Hepbasli. Exergoeconomic, sustainability and environmental damage cost analyses of T56 turboprop engine, Energy 64(2014) 582-600.
http://dx.doi.org/10.1016/j.energy.2013.09.066.

[10] H. Aydın, T. Önder, H. T. Karako, A. Midilli. Exergo-sustainability indicators of a turboprop aircraft for the phases of a flight. Energy58 (2013) 550-560.
http://dx.doi.org/10.1016/j.energy.2013.04.076.

[11] M. Haroon, N.A Sheikh, A. Ayub, R. Tariq, F. Sher, A. T. Baheta, M. Imran. Exergetic, economic and exergo-environmental analysis of bottoming power cycles operating with CO2-based binary mixture. Energies 13(2020) 5080.

[12] A. Midilli, I. Dincer. Development of some exergetic parameters for PEM fuel cells for measuring environmental impact and sustainability. Inter J H Energy 34 (2009) 3858–3872.

[13] M. Jankowski, A. Borsukiewicz. A Novel Exergy Indicator for Maximizing Energy Utilization in Low-Temperature ORC. Energies 13(2020)1598; doi: 10.3390/en13071598.

[14] F.I Abam, E. B Ekwe, S.O Effiom, M.C Ndukwu, T.A Briggs, C.H Kadurumba,. Optimum exergetic performance parameters and thermo-sustainability indicators of low temperature modified organic Rankine cycles (ORCs). Sustainable Energy Technology and Assessments 30(2018)91-104.

[15] P. Ifaei, A. Ataei, C. Yoo. Thermoeconomic and environmental analyses of a low water consumption combined steam power plant and refrigeration Chillers-Part 2: Thermoeconomic an environmental analysis 2016, Energy Convers Manage, http://dx.doi.org/10.1016/j.enconman.2016.06.030.

[16] T. Karakoc, H. Aydin, O. Turan, A. Midilli. Exergo-Sustainability Indicators of a Turboprop Aircraft for the Phases of a Flight, Energy 58(2013) 550-560.

[17] M. C. Ndukwu, F. I. Abam, S. I. Manuwa, T. A. Briggs. Exergetic performance indicators of a direct evaporative cooling system with different evaporative cooling pads. Inter J. of Ambient Energy.38 (7) (2017)701-709
http://dx.doi.org/10.1080/01430750.2016.1195774

[18] M. Cardu, M. Baica. Regarding a global methodology to estimate the energy-ecologic efficiency of thermo power plants. Energy Conver Manage 40(1999) 71-87.

[19] C. F. Santos, R. F. Paulino, C. E. Tuna, J. L. Silveira, F. H. Araújo. Thermodynamic analysis and ecological efficiency of a combined cycle power plant. Thermal Engineering, 13:2(2014) 03-08.

[20] F.I Abam, T.A.Briggs, E. O. Diemuodeke, B.E. Ekwe, K.N Ujoatuonu, J. Isaac, M.C Ndukwu. Thermodynamic and economic analysis of a Kalina system with integrated lithium-bromide-absorption cycle for power and cooling production. Energy Rep 6 (2020) 1992–2005.

[21] C. Hwang, K. Yoon, K. (1981). Multiple Attribute Decision Making Methods and Applications: A State-of-the-Art Survey (1st Edn.). Berlin Heidelberg New York: Springer-Verlag (1981).

[22] G. O. Odu. Weighting Methods for Multi-Criteria Decision Making Technique. J. Appl. Sci. Environ. Manage, 23(8) (2019)1449-1457.

[23] F.I. Abam, D.C Onyejekwe, G.O Unachukwu. The effect of ambient temperature on components performance of an in-service gas turbine plant using exergy method. Singapore Journal of Scientific Research 1(1)(2011)23-37.


This article is an open-access article distributed under the terms and conditions of the Creative Commons Attribution (CC BY) license (https://creativecommons.org/licenses/by/4.0/).